

Temperature-dependent Gilbert damping in Co_2FeAl thin films with different B2 ordering degrees

Gesang Dunzhu(格桑顿珠), Yi-Bing Zhao(赵逸冰), Ying Jin(金莹), Cai Zhou(周偲), and Chang-Jun Jiang(蒋长军)

Citation: Chin. Phys. B, 2020, 29 (**12**): 126701. DOI: 10.1088/1674-1056/abb231
Journal homepage: http://cpb.iphy.ac.cn; http://iopscience.iop.org/cpb

What follows is a list of articles you may be interested in

Crystal structure and electromagnetic responses of tetragonal GdAlGe

Cong Wang(王聪), Yong-Quan Guo(郭永权)†, Tai Wang(王泰), and Shuo-Wang Yang(杨硕望)
Chin. Phys. B, 2020, 29 (**12**): 127502. DOI: 10.1088/1674-1056/abad25

Critical behavior in the layered organic-inorganic hybrid $(CH_3NH_3)_2CuCl_4$

Tina Raoufi, Yinina Ma(马怡妮娜), Young Sun(孙阳)
Chin. Phys. B, 2020, 29 (**6**): 067503. DOI: 10.1088/1674-1056/ab892c

Influence of additives on the magnetic damping constant of CoIr soft magnetic thin films with negative magnetocrystalline anisotropy

Tianyong Ma(马天勇), Zhi Luo(罗智), Zhiwei Li(李志伟), Liang Qiao(乔亮), Tao Wang(王涛), Fashen Li(李发伸)
Chin. Phys. B, 2019, 28 (**5**): 057505. DOI: 10.1088/1674-1056/28/5/057505

Effects of chemical pressure on diluted magnetic semiconductor $(Ba,K)(Zn,Mn)_2As_2$

Y Peng(彭毅), S Yu(于爽), G Q Zhao(赵国强), W M Li(李文敏), J F Zhao(赵建发), L P Cao(曹立朋), X C Wang(望贤成), Q Q Liu(刘清青), S J Zhang(张思佳), R Z Yu(于润泽), Z Deng(邓正), X H Zhu(朱小红), C Q Jin(靳常青)
Chin. Phys. B, 2019, 28 (**5**): 057501. DOI: 10.1088/1674-1056/28/5/057501

Sm–Co high-temperature permanent magnet materials

Shiqiang Liu(刘世强)
Chin. Phys. B, 2019, 28 (**1**): 017501. DOI: 10.1088/1674-1056/28/1/017501

Temperature-dependent Gilbert damping in Co_2 FeAl thin films with different B2 ordering degrees*

Gesang Dunzhu(格桑顿珠)[1], Yi-Bing Zhao(赵逸冰)[2], Ying Jin(金莹)[2], Cai Zhou(周偲)[3,†], and Chang-Jun Jiang(蒋长军)[2,‡]

[1] Science and Technology on Vacuum Technology and Physics Laboratory, Lanzhou Institute of Physics, Lanzhou 730000, China
[2] Key Laboratory for Magnetism and Magnetic Materials, Ministry of Education, Lanzhou University, Lanzhou 730000, China
[3] Hubei Province Engineering Research Center for Intelligent Micro-nano Medical Equipment and Key Technologies, School of Electrical and Electronics Engineering, Wuhan 430200, China

(Received 17 May 2020; revised manuscript received 5 August 2020; accepted manuscript online 25 August 2020)

The temperature-dependent Gilbert damping in Co_2FeAl thin film grown on a $Pb(Mg_{1/3}Nb_{2/3})O_3$-30%$PbTiO_3$ substrate is investigated by the systematic measurement of physical property measurement system (PPMS) on a series of samples with different substrate temperatures. Varying the substrate temperatures from 350 °C to 500 °C, the B2 ordering degrees of Co_2FeAl thin films increase, which can lead the Gilbert damping to decrease, indicated by the field-sweep in-plane PPMS measurements. In addition, the measurement result of PPMS demonstrates that the Gilbert damping decreases first with measurement temperature decreasing down to about 150 K, then increases at a measurement temperature of ∼ 50 K, and decreases again with the measurement temperature decreasing. There are two independent damping manners, namely bulk damping and surface damping, which contribute to the Gilbert damping. Moreover, the observed peak of Gilbert damping at ∼ 50 K can be attributed to the spin re-orientation transition at the Co_2FeAl surface, which is similar to the result of the effective magnetization as a function of measurement temperature. The result presents the evidence for further studying the Gilbert damping in Co_2FeAl thin film.

Keywords: Gilbert damping, Co_2FeAl thin film, B2 ordering degree

PACS: 67.30.er, 67.80.dk, 75.50.–y, 62.25.Fg **DOI:** 10.1088/1674-1056/abb231

1. Introduction

The magnetic material for applications in magnetic storage devices with high-speed and low-power consumption is usually based on the analysis of magnetization dynamics subjected to a phenomenological parameter called Gilbert damping α as given by the Landau–Lifshitz–Gilbert (LLG) equation[1–8]

$$\frac{\mathrm{d}}{\mathrm{d}t}\boldsymbol{M} = -\gamma \boldsymbol{M} \times \boldsymbol{H}_{\mathrm{eff}} + \frac{\alpha}{M_{\mathrm{s}}} \boldsymbol{M} \times \frac{\mathrm{d}}{\mathrm{d}t}\boldsymbol{M}, \tag{1}$$

where γ is the gyromagnetic ratio, $\boldsymbol{M}$ is the magnetization vector, and M_{s} is the saturation magnetization. According to the LLG equation, the Gilbert damping α is particularly important for controlling how the magnetization rapidly reaches the equilibrium position without the external stimulus, and for describing the magnetic dynamic property in the magnetic thin film. Generally, the magnetization dynamics can be governed by intrinsic and extrinsic contributions. The former is determined by the fundamental material parameter, α for a ferromagnet describing the rate of magnetization relaxation, which can be obtained to perform the measurements under different values of frequency f due to α proportional to f. The latter counterpart is characterized by the magnon excitations and magnetic film inhomogeneity. A low α in ferromangnetic material can lead to a low critical current density, which can be implemented in spin-transfer-torque magnetic random access memories. The Co_2FeAl (CFA) material due to high Currie temperature, high spin polarization, especially a low α, is chosen, which has been a hot research spot in this field. The theoretical and experimental approaches have been employed to study Gilbert damping α in CFA material. For instance, Belmeguenai *et al*. have reported the experimentally derived α, obtained by linearly fitting the curve of frequency-dependent ferromagnetic resonance linewidth, which varies from 0.0068 to 0.00154 with CFA thickness changing from 10 nm from 70 nm in CFA/MgO structure.[9] In addition, the chemical order varies from A2 phase to B2 phase with thickness increasing. Therein, A2 phase has a completely random occupation for any Co, Fe, or Al atom, and B2 phase has Co atoms occupying their assigned sites, while Fe and Al atoms randomly share the other ones. Husain *et al*. have investigated that the static and dynamic magnetization properties in the B2 phase CFA thin film grown at different values of Si substrate temperature T_{s}.[10] A low α of 0.0015±0.0001 is ob-

*Project supported by the National Natural Science Foundation of China (Grant Nos. 51671099, 11974149, and 51901163) and the Program for Changjiang Scholars and Innovative Research Team in University, China (Grant No. IRT-16R35).

†Corresponding author. E-mail: szhou@wtu.edu.cn
‡Corresponding author. E-mail: jiangchj@lzu.edu.cn

© 2020 Chinese Physical Society and IOP Publishing Ltd

tained corresponding to T_s of $\sim$ 573 K. To realize the potential applications of CFA thin film, the ordering degree and low-α CFA prepared by controlling the growth conditions and choosing the substrate is essential. Recently, with the continuous development of many existing and emerging devices such as magnetic random access memories, a particular ferroelectric crystal material $Pb(Mg_{1/3}Nb_{2/3})O_3$-30%$PbTiO_3$(PMN-PT) is often used in the multiferroelectric heterostructures. In previous reports,[11,12] the magnetic dynamic and ferromagnetic resonance linewidth in a fixed microwave frequency can be obtained in CFA/PMN-PT structure. Nevertheless, the orderiomng degree of CFA grown on PMN-PT substrate is ignored, and α is unsolved. Therefore, in this work, the temperature-dependent Gilbert damping in CFA thin film grown on ferroelectric crystal material PMN-PT is analyzed in detail. With the substrate temperature varying from 350 °C to 500 °C, the B2 ordering degree of CFA thin film increases, which can lead the Gilbert damping to decrease, indicated by the field-sweep in-plane physical property measurement system (PPMS) measurements. Therein, the resonance spectra are obtained by the PPMS measurements at temperatures in a range of 5 K–300 K and frequencies in a range of 8 GHz–17 GHz. The Gilbert damping is also found to decrease with measurement temperature decreasing, and then to increase with measurement temperature decreasing down to about 50 K followed by decreasing again, which can be attributed to the two independent contributions, namely bulk damping and surface damping. Moreover, an abnormal point of the effective magnetization around $\sim$ 50 K is obtained, which is consistent with the results of Gilbert damping at different measurement temperatures. This can result from the spin reorientation transition at the CFA surface.

2. Experiment

The CFA thin film was deposited on the (001)-oriented PMN-PT ($Pb(Mg_{1/3}Nb_{2/3})O_3$-$PbTiO_3$) substrate by direct current (DC) magnetron sputtering under different values of substrate temperature T_s: 350 °C, 400 °C, 450 °C, and 500 °C, respectively. The sputtering condition included an Ar pressure of 0.1 Pa, a flow rate at 10 SCCM (SCCM denotes cubic centimeter per minute at STP), and a base pressure of 2×10^{-5} Pa. The sputtering power was 180 W, and the thickness values of CFA thin films are all 150 nm. The x-ray diffraction (XRD) measurement was performed on X'Pert x-ray powder diffractometer with Cu-$K\alpha$ radiation (1.54056 Å). After the XRD measurement, Pt layers were sputtered on the top side and bottom side, respectively, with thickness being 10 nm and 50 nm. The Pt layer was used as an electrode when the sample was measured by PPMS. The Keithley 2400 source measurement unit was used to test the resistance of the sample through using the four-probe technique. The temperature dependence of the ferromagnetic resonance absorption spectrum was measured with a physical property measurement system (PPMS) possessing a broadband ferromagnetic resonance setup, by using a coplanar waveguide for microwave excitation and operating in a frequency range of 2 GHz–18 GHz. The setup is also used with a temperature control system operating from 1.9 K to 400 K.

3. Results and discussion

The XRD patterns of CFA thin films with different values of T_s during deposition are shown in Fig. 1(a). The CFA thin films are deposited at T_s = 350 °C, 400 °C, 450 °C, and 500 °C and the corresponding samples are named S350, S400, S450, and S500, respectively. For the S400, the (400) fundamental peak is observed obviously at $\sim$65.09° in this film, which originates from the basic cubic crystal structure, corresponding to the A2 phase of CFA. The A2 phase is totally disordered with respect to Co, Fe, and Al. The presence of (200) peak at $\sim$ 31.19° indicates that the sample contains B2 phase. The B2 phase is characterized by total disorder between Fe and Al atoms while Co atoms occupy regular sites. A similar behavior can be obtained for samples S450 and S500, respectively, which suggests the appearance of B2 phase. For the S350, there is no (200) peak corresponding to the CFA phase detected in XRD scans, which only can be defined as A2 phase. However, with the accuracy of the measurements, the $L2_1$-type peak at approximate 27° cannot be observed. The ratio of integrated intensity of (002) peak to that of (004) peak ($I_{(002)}/I_{(004)}$) as shown in the blue curve of Fig. 1(b) increases with T_s increasing from 350 °C to 500 °C, which demonstrates the improvement of the B2 phase ordering degree. Moreover, to quantify the chemical ordering of B2 phase, the parameter (S_{B2}) is given as follows:[13]

$$\frac{I_{(200)}}{I_{(400)}} = S_{B2}^2 \left(\frac{I_{(200)}^{\text{full-order}}}{I_{(400)}^{\text{full-order}}} \right), \tag{2}$$

where $I_{(200)}^{\text{full-order}}/I_{(400)}^{\text{full-order}}$ is the ideal ratio between the two peaks. The S_{B2} parameter for S350, S450, and S500 can be obtained from Eq. (2), which is shown by the red curve in Fig. 2(b). The S_{B2} parameter increases from 0.34% to 0.53% with T_s increasing from 400 °C to 500 °C. These results indicate that the highest-ordered CFA thin films in this work can be achieved for the S500, which may be explained qualitatively in the following. As the substrate temperature increases, the increase of the atom ordering degree leads the ordering phase to increase.

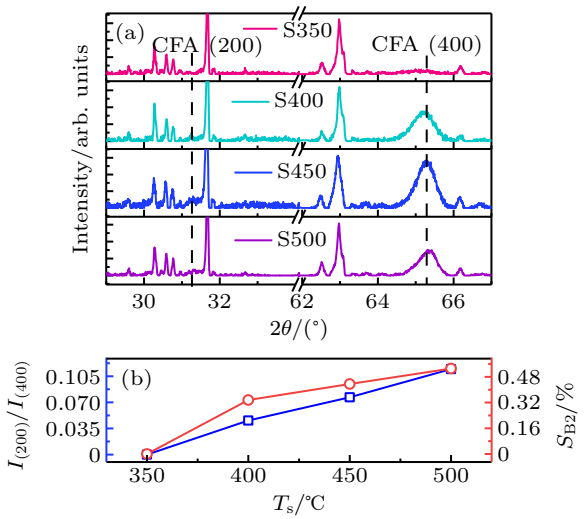


Fig. 1. (a) XRD patterns of CFA/PMN-PT heterostructure at different substrate temperatures T_s and (b) T_s-dependent $I_{(200)}/I_{(400)}$ and S_{B2}.

Besides the result measured by XRD, the anisotropy magnetoresistance (AMR) can also be a fingerprint for half-metallic/non-half-metallic material.[14,15] The AMR is measured by using a homemade measurement system. The current 0.8 mA and magnetic field 1000 Oe (1 Oe = 79.5775 A·m^{-1}) are applied to these samples. The $[(\rho(\varphi_H)\rho_\perp)/\rho_\perp]\times 100\%$ of the CFA thin film as a function of φ_H (the direction of in-plane applied magnetic field H with respect to the [100] direction of PMN-PT) can be obtained. The curve of $[(\rho(\varphi_H)\rho_\perp)/\rho_\perp]\times 100\%$ *versus* φ_H for S350, S450, and S500 are shown in Fig. 2, which show the clear twofold symmetry. For the S350, the sign of the $[(\rho(\varphi_H)\rho_\perp)/\rho_\perp]\times 100\%$ tends to be positive, which can be attributed to the dominant s–d scattering process from up-spin s-state to down-spin d-states (s ↑→ d ↓) or s ↓→ d ↑. However, for the S450 and S500, the $[(\rho(\varphi_H)\rho_\perp)/\rho_\perp]\times 100\%$ is negative due to the dominant scattering process s ↑→ d ↑ or s ↓→ d ↓, which is in agreement with that in Fe_4N and $Co_2Fe_xMn_{1-x}Si$ thin film. Therefore, the result proves the half-metallic character of CFA thin film for the S450 and S500. Moreover, with T_s increasing from 350 °C to 500 °C, the AMR ratio (defined as $[(\rho_\parallel-\rho_\perp)/\rho_\perp]\times 100\%$) decreases from 0.0914% to −0.1023%, indicating the increase of B2 phase ordering degree, which is consistent with the result measured by XRD.

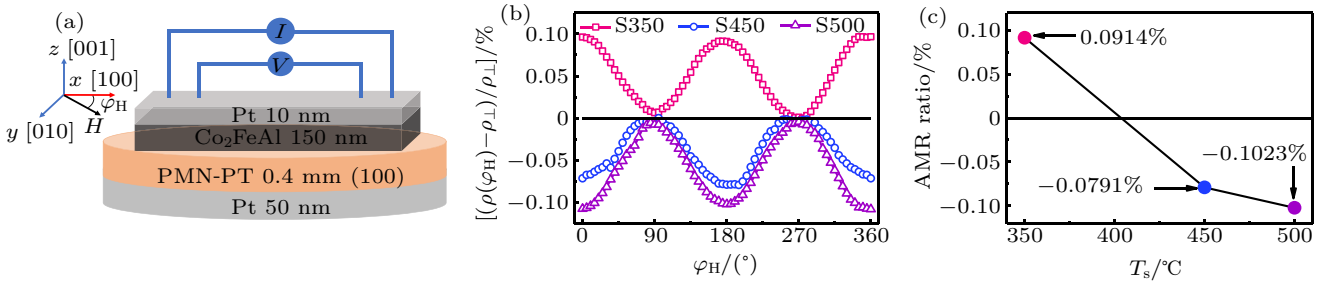


Fig. 2. (a) Schematic diagram of AMR measurement. (b) $[(\rho(\varphi_H)-\rho_\perp)/\rho_\perp]\times 100\%$ *versus* angle between magnetic field and applied current direction for S350, S450, and S500. (c) AMR ratio (defined as $[(\rho_\parallel-\rho_\perp)/\rho_\perp]\times 100\%$) *versus* T_s for S350, S450, and S500.

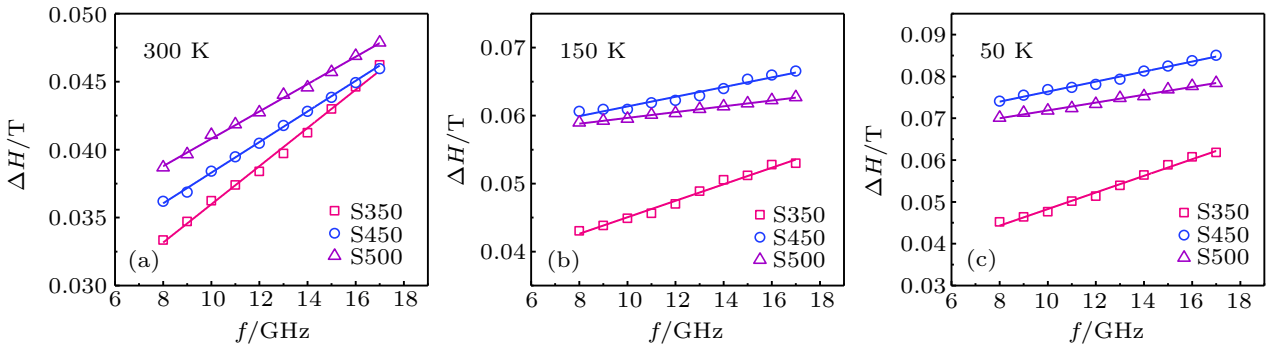


Fig. 3. Curves of ΔH *versus* f for samples S350, S450, and S500 at measurement temperature: (a) 300 K, (b) 150 K, and (c) 50 K, respectively.

To investigate the temperature-dependent Gilbert damping and the effective magnetization, these samples are measured by PPMS at measurement temperature T_{mm} ranging from 1.4 K to 300 K and frequency f in a range from 8 GHz to 17 GHz. The PPMS mainly consists of a vector-network analyzer using a coplanar waveguide, and a conventional method using phase-ferromagneti-resonance.[16–18] The radio-frequency microwave magnetic field is transmitted along the coplanar waveguide, which can be regarded as perturbation to induce the magnetiztaion precession of the sample placed on the coplanar waveguide. The phase-ferromagneti-resonance is characterized by the measurement of sweeping-field ferromagnetic-resonance at any fixed microwave frequency, and the lock-in and Helmholtz coils are added to improve the accuracy of signal. As shown in Fig. 4(a), these integral curves at $T_m = 300$ K and the frequency $f = 11$ GHz for

samples S350, S450, and S500 can be obtained. The applied magnetic field is along the direction [110]/[-1-10] of PMN-PT. The actual function of the absorption curve is given by an asymmetric Lorentzian function[19]

$$\xi(H) = A\frac{\Delta H\cos\delta + (H - H_{\rm r})\sin\delta}{\Delta H^2 + (H - H_{\rm r})^2}, \tag{3}$$

where H is the external magnetic field, $H_{\rm r}$ is the magnetic resonance field, ΔH is the half-width at half-maximum of the linewidth, δ is the phase that mixes the real part and imaginary part of the dynamic susceptibility, and A is the integral coefficient. The value of ΔH can be obtained by fitting these integral curves according to Eq. (3).

The curves of the extracted ΔH *versus* f for the corresponding samples are shown in Fig. 3. For brevity, only data at $T_{\rm m} = 50$ K, 150 K, and 300 K are plotted. ΔH has the linear change with f from 8 GHz to 17 GHz, for which these curves can be fitted by the following equation[20]

$$\Delta H = \Delta H_0 + \frac{4\pi}{\gamma}\alpha f, \tag{4}$$

where ΔH_0 is the frequency-independent contribution from the sample inhomogeneity, which can result from the dispersion distribution of magnetization and magnetic inhomogeneity in single-layered ferromagnetic thin film; and the second term on the right-hand side corresponds to the frequency-dependent contribution associated with the intrinsic Gilbert damping α. As shown in Fig. 3(a), at $T_{\rm m} = 300$ K, ΔH for the S500 is larger than that for the S450. However, at $T_{\rm m} = 150$ K and 50 K, ΔH values for the S450 are larger than those for the S500, which can be attributed to the substrate temperature $T_{\rm s}$ of 450 °C close to the phase temperature between A2 phase and B2 phase of CFA material, leading the defects induced by impurities, interface and electron holes to increase and also the inhomogeneity of magnetization to augment. The curves of ΔH *versus* f can be fitted by Eq. (4). Meanwhile, the intrinsic Gilbert damping α under different values of $T_{\rm m}$ can be obtained for S350, S450, and S500, which is shown in Fig. 5(b). At each value of $T_{\rm m}$, the lowest Gilbert damping appears in the S500 thin film with a highest B2 ordering degree. With the gradual decrease of the B2 ordering degree in samples S450 and S350 obtained by the result of XRD as shown in Fig. 1(a), the Gilbert damping increases, which can be attributed to the density of states at Fermi level. Interestingly, for the three samples S500, S450, and S350, the Gilbert damping decreases monotonically as the $T_{\rm m}$ decreases from 300 K to 150 K, which is expected in bulk materials due to suppressing the scattering. As the $T_{\rm m}$ continues to decrease, an enhanced peak of the damping is observed at $T_{\rm m} \sim 50$ K. With $T_{\rm m}$ decreasing further, the Gilbert damping decreases again. For the S350, the Gilbert damping shows a slight decrease first from 0.0189 at 300 K to 0.0158 at 150 K, and a giant enhancement up to 0.0245 at 50 K, and then a sharp decrease down to 0.0155 at 5 K. A similar behavior can be observed for samples S450 and S500. From the temperature dependence, two independent contributions to the Gilbert damping are pointed out, namely bulk damping and surface damping.[21] The bulk damping decreases monotonically as the temperature decreases, while the surface damping shows an enhancement peak at $T_{\rm m} \sim 50$ K.

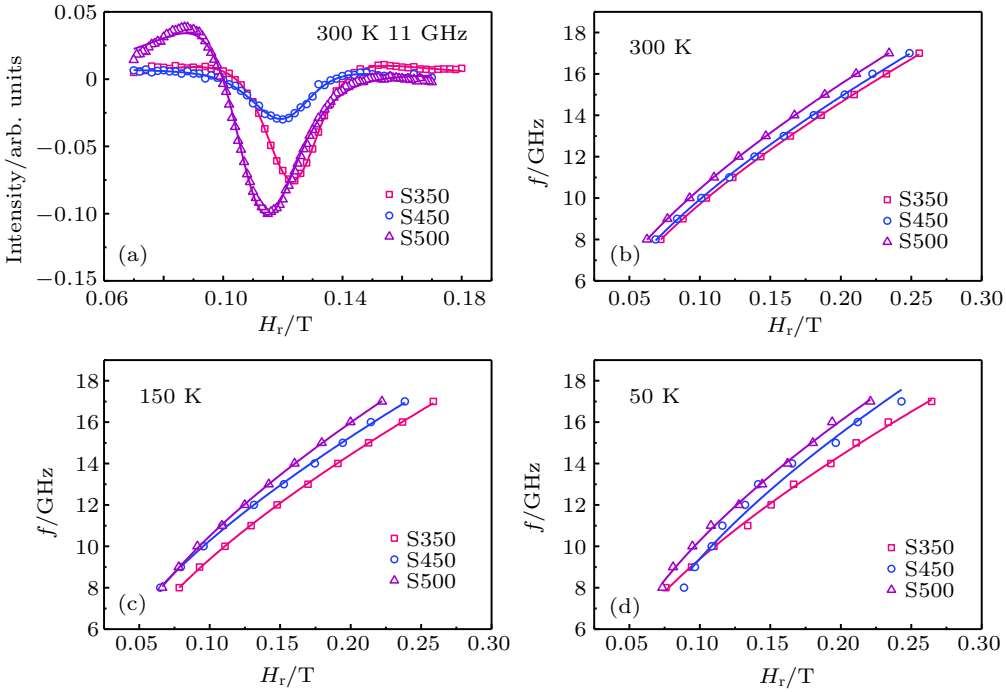


Fig. 4. (a) Ferromagnetic resonance absorption spectra for samples S350, S450, and S500 at measurement temperature 300 K and frequency 11 GHz. Curves of f *versus* $H_{\rm r}$ for samples S350, S450, and S500 at measurement temperature (b) 300 K, (c) 150 K, and (d) 50 K, respectively.

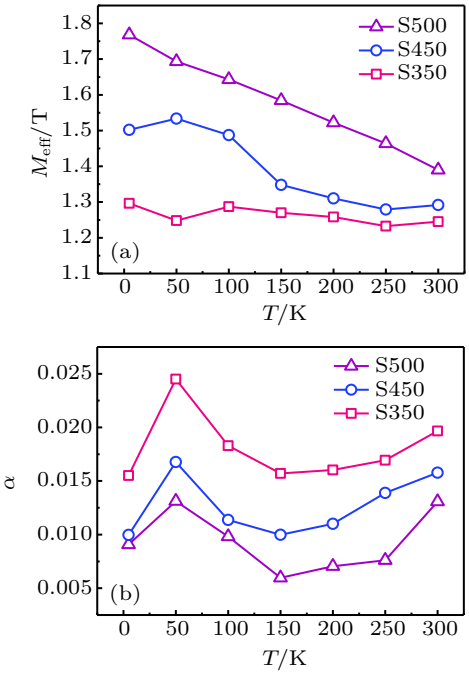


Fig. 5. (a) Curves of effective magnetization *versus* measurement temperature for samples S350, S450, and S500, respectively. (b) Curves of Gilbert damping *versus* measurement temperature for samples S350, S450, and S500, respectively.

The possible mechanism for the observed peak of the Gilbert damping at $T_{\rm m} \sim 50$ K could be related to a thermally induced spin re-orientation transition on the Co_2FeAl surface at that temperature. The curves of f *versus* $H_{\rm r}$ at $T_{\rm m} = 300$ K respectively for S350, S450, and S500 are shown in Fig. 4(b). The similar results at $T_{\rm m} = 150$ K and 50 K are shown in Figs. 4(c) and 4(d), respectively. For brevity, only data at $T_{\rm m} = 50$ K, 150 K, and 300 K are plotted. At the fixed $T_{\rm m}$ and f, $H_{\rm r}$ decreases with the increase of substrate temperature $T_{\rm s}$, which can be attributed to the saturation magnetization and magnetic anisotropy varying with $T_{\rm s}$. The effective magnetization $M_{\rm eff}$ is estimated from the curves of f *versus* $H_{\rm r}$ at various values of $T_{\rm m}$ by using the in-plane Kittel's equation[20]

$$f = \frac{\gamma}{2\pi}\sqrt{H_{\rm r}(H_{\rm r}+M_{\rm eff})}. \tag{5}$$

The $M_{\rm eff}$ contains the saturation magnetization and the other anisotropy contributions. The plots of $T_{\rm m}$ dependence of $M_{\rm eff}$ for S350, S450, and S500 in Co_2FeAl films are shown in Fig. 5(a). At each value of $T_{\rm m}$, $M_{\rm eff}$ increases with $T_{\rm s}$ increasing. For example, at $T_{\rm m} = 300$ K, $M_{\rm eff}$ increases from 1.25 T to 4.00 T with $T_{\rm s}$ increasing from 350 °C to 500 °C. The effective magnetization for S500 seems to have an almost linear change of the effective magnetization with measurement temperature. In fact, the anomaly of effective magnetization at ~ 50 K is not excepted. However, an obvious anomaly in the effective magnetization for the thin film (S350 and S450) is obtained, which can be attributed to the thermally-induced SRT in CFA thin film.[22,23] Nevertheless, the underlying mechanisms of the enhancement peak of surface damping and the effective magnetization at the measuremnt temperature of 50 K should be further investigated in future.

4. Conclusions

In this work, the temperature dependence of Gilbert damping in Co_2FeAl thin film grown on a PMN-PT substrate is investigated. The B2 ordering degree of Co_2FeAl thin film grown on a PMN-PT substrate can be obtained. The B2 ordering degree increases with substrate temperature increasing, which can lead the Gilbert damping to decrease. Moreover, a relatively low Gilbert damping 0.006 can be found at 150 K. With the measurement temperature varying from 5 K to 400 K, an enhancement peak of Gilbert damping appears at ~ 50 K, which can be attributed to the spin re-orientation for the surface magnetization of Co_2FAl thin film. This can be proved by an enhancement of the effective magnetization at ~ 50 K. The result adds the evidence for further studying the Gilbert damping in Co_2FeAl thin film.

References

[1] Schoen M A W, Thonig D, Schneider M L, Silva T J, Nembach H T, Eriksson O, Karis O and Shaw J M 2016 *Nat. Phys.* **12** 839

[2] Chen H, Fan X L, Wang W X, Zhou H A, Gui Y S, Hu C M and Xue D S 2013 *Appl. Phys. Lett.* **102** 202410

[3] Wang G X, Dong C H, Jiang C J, Chai G Z and Xue D S 2012 *J. Magn. Magn. Mater.* **324** 2840

[4] Lenz K, Wende H, Baberschke K, Nagy K and Jánossy A 2006 *Phys. Rev. B* **73** 144424

[5] Tserkovnyak Y, Brataas A and Bauer G E W 2002 *Phys. Rev. B* **88** 117601

[6] Mizukami S, Ando Y and Miyazaki T 2002 *Phys. Rev. B* **66** 104413

[7] Urban R, Woltersdorf G and Heinrich B 2001 *Phys. Rev. Lett.* **87** 217204

[8] Lakshmanan M and Nakamura K 1984 *Phys. Rev. Lett.* **53** 2497

[9] Belmeguenai M, Tuzcuoglu H, Gabor M S, Petrisor T Jr, Tiusan C, Zighem F, Chérif S M and Moch P 2014 *J. Appl. Phys.* **115** 043918

[10] Husain S, Akansel S, Kumar A, Svedlindh P and Chaudhary S 2016 *Sci. Rep.* **6** 28692

[11] Zhou C, Dunzhu G S, Yao J L and Jiang C J 2017 *J. Alloys Compd.* **710** 680

[12] Zhou C, Wang F L, Dunzhu G S, Yao J L and Jiang C J 2016 *J. Phys. D: Appl. Phys.* **49** 455001

[13] Okamura S, Miyazaki A, Tezuka N, Sugimoto S and Inomata K 2006 *Mater. Trans.* **47** 15

[14] Yang F J, Sakuraba Y, Kokado S, Kota Y, Sakuma A and Takanashi K 2012 *Phys. Rev. B* **86** 020409

[15] Yang F J, Wei C and Chen X Q 2013 *Appl. Phys. Lett.* **102** 172403

[16] Kumar A, Pan F, Husain S, Akansel S, Brucas R, Bergqvist L, Chaudhary S and Svedlindh P 2017 *Phys. Rev. B* **96** 224425

[17] Wu Y, Zhao Y L, Xiong Q, Xu X G, Sun Y, Zhang S Q and Jiang Y 2014 *Chin. Phys. B* **23** 018503

[18] Wang N, Jin Y R, Deng H, Wu Y L, Zheng G L, Li S, Tian Y, Ren Y F, Chen Y F and Zheng D N 2012 *Acta. Phys. Sin.* **61** 213302 (in Chinese)

[19] Farle M 1998 *Rep. Prog. Phys.* **61** 755

[20] Husain S, Kumar A, Barwal V, Behera N, Akansel S, Svedlindh P and Chaudhary S 2018 *Phys. Rev. B* **97** 064420

[21] Zhao Y L, Song Q, Yang S H, Su T, Yuan W, Patkin S S P, Shi J and Han W 2016 *Sci. Rep.* **6** 22890

[22] Sierra J F, Pryadum V V, Russek S E, García-HernÁndez M, Mompean F, Rozada R, Chubykalo-Fesenko O, Snoeck E, Miao G X, Moodera J S and Aliev F G 2011 *J. Nanosci. Nanotechnol.* **11** 7653

[23] Zhao Y L, Song Q, Yang S H, Su T, Yuan W, Parkin S S P, Shi J and Han W 2016 *Sci. Rep.* **6** 22890